Publ. Astron. Soc. Japan (2018) 70 (5), 95 (1–9)
doi: 10.1093/pasj/psy093
Advance Access Publication Date: 2018 September 11

Discovery and state transitions of the new Galactic black hole candidate MAXI J1535−571

Satoshi Nakahira,[1] Megumi Shidatsu,[1,2] Kazuo Makishima,[1] Yoshihiro Ueda,[3] Kazutaka Yamaoka,[4] Tatehiro Mihara,[1] Hitoshi Negoro,[5] Tomofumi Kawase,[5] Nobuyuki Kawai,[6] and Kotaro Morita[6]

[1]MAXI team, RIKEN, 2-1 Hirosawa, Wako, Saitama 351-0198, Japan
[2]Department of Physics, Ehime University, 2-5 Bunkyocho, Matsuyama, Ehime 790-8577, Japan
[3]Department of Astronomy, Kyoto University, Kitashirakawa-Oiwake-cho, Sakyo-ku, Kyoto, Kyoto 606-8502, Japan
[4]Institute for Space-Earth Environmental Research (ISEE), Nagoya University, Furo-cho, Chikusa-ku, Nagoya, Aichi 464-8601, Japan
[5]Department of Physics, Nihon University, 1-8 Kanda-Surugadai, Chiyoda-ku, Tokyo 101-8308, Japan
[6]Department of Physics, Tokyo Institute of Technology, 2-12-1 Ookayama, Meguro-ku, Tokyo 152-8551, Japan

Received 2018 April 3; Accepted 2018 July 21

Abstract

We report on the detection and subsequent X-ray monitoring of the new Galactic black hole candidate MAXI J1535−571 with the Gas Slit Camera onboard Monitor of All-sky X-ray Image (MAXI/GSC). After the discovery on 2017 September 2, made independently with MAXI and the Swift/BAT, the source brightened gradually, and in a few weeks reached the peak intensity of ∼5 Crab, or $\sim 1.6 \times 10^{-7}$ erg cm^{-2} s^{-1} in terms of the 2–20 keV flux. On the initial outburst rise, the 2–20 keV MAXI/GSC spectrum was described by a power-law model with a photon index of $\lesssim 2$, while after a hard-to-soft transition, which occurred on September 18, the spectrum required a disk blackbody component in addition. At around the flux peak, the 2–8 keV and 15–50 keV light curves showed quasi-periodic and anti-correlated fluctuations with amplitudes of 10%–20%, on a time scale of ∼1 d. Based on these X-ray properties obtained with the MAXI/GSC, with additional information from the Swift/BAT, we discuss the evolution of the spectral state of this source, and give constraints on its system parameters.

Key words: accretion, accretion disks — black hole physics — X-rays: binaries — X-rays: individual (MAXI J1535−571)

1 Introduction

Transient black hole binaries (BHBs) sometimes exhibit dramatic outbursts, changing their X-ray luminosity over several orders of magnitude. Their outburst light curves typically consist of a rapid rise on timescales of a few days to a few weeks, and a subsequent slow decay on timescales of weeks to a few months. In their outbursts, they show distinct "states" with different spectral properties (e.g., Done et al. 2007; McClintock & Remillard 2006). The canonical two states are the so-called hard state and the soft state, where the spectrum below 10 keV is characterized by a hard power-law component with a photon index of <2, and by a multi-color disk blackbody component (Mitsuda et al. 1984), respectively. BHBs are known

to exhibit a hysteresis in their flux versus spectral evolution; they make state transitions from the hard state to the soft state and in the opposite direction at different luminosities, and consequently track a q-shaped curve on an X-ray hardness-intensity diagram (HID: Homan & Belloni 2005). Because the spectral properties are considered to reflect the structure and dynamics of accretion flows in the vicinity of the central black holes, probing the complex spectral evolution during outbursts gives us clues to the physics of black hole accretion over a wide range of mass accretion rates.

MAXI J1535−571 was detected on 2017 September 2 with the Gas Slit Camera (GSC) onboard MAXI (Matsuoka et al. 2009), which is operating on the International Space Station (ISS). The MAXI/GSC nova alert system (Negoro et al. 2016) triggered on the source at UT 14:41 with a low significance. As reported by Negoro et al. (2017a), the detection was confirmed with subsequent scans, which recorded an X-ray intensity of 34 ± 6 mCrab in 4–10 keV. Almost simultaneously and independently, the burst alert telescope (BAT) of the Swift satellite also discovered the source (Kennea et al. 2017; Markwardt et al. 2017), and precisely determined its position at $(\alpha,\ \delta) = (15^{\rm h}35^{\rm m}19\overset{\rm s}{.}73,\ -57^\circ13'48\overset{''}{.}1)$ with the X-ray telescope and ultraviolet/optical telescope onboard. After the discoveries and a gradual increase of the flux, the source spectrum softened on about September 18 (Kennea 2017; Nakahira et al. 2017; Palmer et al. 2017) and a disk blackbody component became significant (Shidatsu et al. 2017), suggesting a state transition from the hard state into the soft state.

Follow-up observations of the object were extensively performed in various wavelengths (Britt et al. 2017; Dincer 2017; Gendreau et al. 2017; Kennea 2017; Mereminskiy & Grebenev 2017; Nakahira et al. 2017; Russell et al. 2017a, 2017b; Scaringi & ASTR211 Students 2017; Shidatsu et al. 2017; Tetarenko et al. 2017). The counterpart of MAXI J1535−571 was found in the optical and infrared bands soon after the onset of the outburst, with a relatively low optical flux (∼21 mag in the i' band; Dincer 2017; Scaringi & ASTR211 Students 2017). Radio emission from the object was also detected (Russell et al. 2017b; Tetarenko et al. 2017). The source was interpreted as a new BH candidate in our galaxy, considering the X-ray spectral shapes and rapid X-ray variability (Negoro et al. 2017b), as well as the radio versus X-ray flux ratio (Russell et al. 2017a). The optical/near-infrared variations suggest that the companion is a low-mass star (Scaringi & ASTR211 Students 2017; Dincer 2017). The nuclear spectroscopic telescope array (NuSTAR) spectrum taken on the fifth day after the outburst onset suggests a low electron temperature, ∼20 keV, and a high spin of $a > 0.84$, assuming the source to be an accreting BH in the hard state (Xu et al. 2018).

As a working hypothesis, we here assume that the object is a new BHB. Based mainly on the MAXI/GSC data, the present paper describes the X-ray behavior of MAXI J1535−571 over the 220 days from the outburst onset.

2 Data analysis and results

2.1 Data reduction

We studied the X-ray properties of MAXI J1535−571 using light curves and spectra obtained with the MAXI/GSC. The 15–50 keV light curve of the Swift/BAT was also employed to investigate the long-term trend in the hard X-ray band.

We analyzed the MAXI data version 1.3.6.6, which is a beta-test version released from the Data ARchive and Transmission System (DARTS) at institute of space and astronautical science of Japan aerospace exploration agency (ISAS/JAXA).[1] Light curves and spectral data were produced from the event data via MAXI-specific tools implemented in the "MAXI/GSC on-demand web interface" (Nakahira et al. 2013).[2] The on-source data were extracted from a circular region with a radius of $2\overset{\circ}{.}1$, centered on the source position. The background data of the same region were produced with a background event generator, which adopts the same method as used in the second MAXI/GSC extragalactic source catalog (Hiroi et al. 2013). To suppress statistical fluctuations, we generated 100 times more background counts than in the real data.

For the Swift/BAT data, we used the archived 15–50 keV light curve with a time resolution of ∼92 min (the spacecraft orbital period), available on the "BAT Transient Monitor" website (Krimm et al. 2013).[3]

2.2 Light curves and hardness ratios

Figure 1 a shows background-subtracted MAXI/GSC light curves of MAXI J1535−571 in 2–8 keV and 8–20 keV, and their hardness ratio (HR). The time origin ($T = 0$ d) was chosen at the onset date of the outburst (= 2017 September 2). Each data point represents one scan transit of the source, which takes place every 92 minutes and lasts for 40–100 s. MAXI was not able to observe the direction of MAXI J1535−571 for $T = 25$–42, $T = 101$–112, 120–121, or 173–182. A Swift/BAT light curve in 15–50 keV is also presented to compare intensity variations at different energies. Because the data with the original sampling are subject to large statistical errors, we took averages typically over 2–20 adjacent data points. These binned data, 114 points in total, are show in red in figure 1a.

The MAXI/GSC light curves and their HRs are converted to an HID in figure 2. There, colored data points represent the binned data in figure 1. Considering the behavior of the

[1] ⟨http://darts.isas.jaxa.jp/astro/maxi/⟩.

[2] ⟨http://maxi.riken.jp/mxondem⟩.

[3] ⟨http://swift.gsfc.nasa.gov/docs/swift/results/transients⟩.

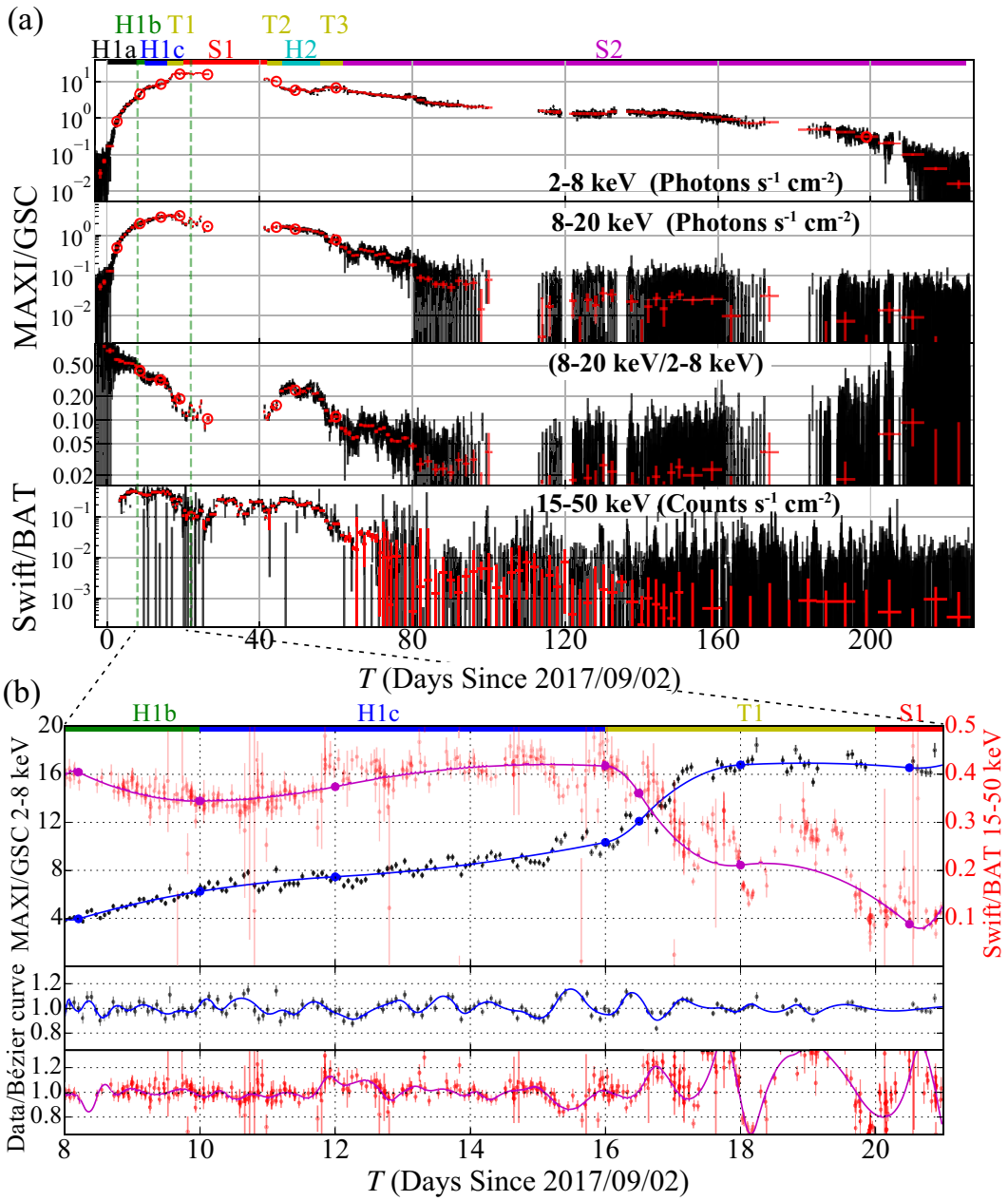

Fig. 1. (a) The MAXI/GSC 2–8 keV and 8–20 keV light curves, hardness ratio between 8–20 keV and 2–8 keV band, and the 15–50 keV Swift/BAT light curve, from top to bottom. Black points indicate data with the finest time resolution (∼92 min), and red points are binned data. (b) Top: the zoomed 2–8 keV (black) and 15–50 keV (red) light curves over the period indicated by a pair of green lines in panel (a), which includes the first hard-to-soft state transition. The second order Bézier curves (solid lines) and its knots (circles) are superposed on the data. Middle and bottom: the ratios of the data to the Bézier curve. Errors in all panels represent 1σ confidence intervals.

light curves and HID with MAXI, the entire outburst period can be classified into the following nine phases. Among them, H1 and H2 represent a relatively hard phase typical of the hard state, S1 and S2 represent relatively soft phases to be interpreted as the soft state, and T1–T3 are transient periods.

H1a (T = 0–8): the 2–8 and 8–20 keV intensities steadily increased, keeping an approximately constant HR ∼0.6.

H1b (T = 8–10): the 2–8 keV flux increased more rapidly than in H1a, and accordingly the HR rapidly declined to ∼0.35.

H1c (T = 10–16): the fluxes in both bands again increased steadily, with a slight decrease of the HR.

T1 (T = 16–20): the source declined rapidly in 2–8 keV and brightened in 8–20 keV simultaneously; this is regarded as the first hard-to-soft state transition.

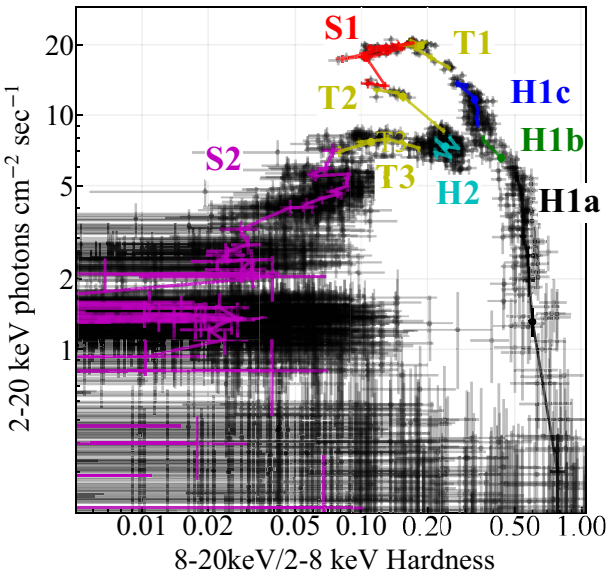

Fig. 2. Scatter plot, namely an HID, between the hardness ratio vs. 2–20 keV intensity of the MAXI/GSC data with the 92-min time resolution. Color points connected with lines are binned data produced in the same manner as in figure 1a. (Color online)

S1 ($T = 20$–42): the 2–8 keV flux was kept at the maximum level, while the 8–20 keV flux gradually decreased with small fluctuations (see below). The HR reached 0.1–0.2, the lowest value of the first portion in the HID.

T2 ($T = 42$–46): the HR rapidly increased, and the source returned to the hard state.

H2 ($T = 46$–56): the HR remained relatively constant, and the source made the second hard-to-soft state transition.

T3 ($T = 56$–62): the HR rapidly decreased.

S2 ($T = 62$–): the 2–8 and 8–20 keV fluxes both decreased steadily, while the HR marked the minimum value in the outburst, ~0.01. Then, after $T = 200$, the source declined more rapidly, keeping the soft spectrum.

The behavior of the 15–50 keV flux was different from that in 8–20 keV; it decreased in H1b and then rose again in H1c. After the rapid decrease at the beginning of T1, it jumped among a few rather discrete intensity levels, and then gradually decreased during H2, T3, and S2 to undetectable levels.

Around $T = 8$–20, the MAXI and Swift data were found to scatter much more than the statistical errors on a timescale of ~ one day. Figure 1b shows an expanded light curve for $T = 8$–22, where a smoothed light curve produced using the second order Bézier curve is superposed. Anti-correlated oscillations can be seen between the 2–8 keV and 15–50 keV intensities with an amplitude of ~10%–20% and a period of ~ one day.

2.3 Energy spectra

We extracted time-averaged MAXI/GSC spectra of MAXI J1535−571 from the 114 binned time points (defined in subsection 2.2). The derived spectra were then fitted with the standard X-ray emission model for BH X-ray binaries: a disk blackbody emission and its Comptonization, both absorbed by cold interstellar plus circum-source medium. We adopted the multi-color disk model `diskbb` (Mitsuda et al. 1984), and convolved it with `simpl` (Steiner et al. 2009) in which a fraction of the input seed photons are redistributed by Comptonization into a power-law form. The absorption was expressed by the `TBabs` model, referring to the solar-abundance table given by Wilms et al. (2000). Because `simpl` is a convolution model, the energy band used in the spectral fitting was extended down to 0.01 keV and up to 100 keV. The spectral analysis was carried out with XSPEC version 12.9.1, and the errors represent 90% confidence limits.

In the fitting, the absorption column density was fixed at $N_{\rm H} = 2.6 \times 10^{22}$ cm^2, a value which was favored by essentially all the spectra. We fixed Γ at 2.50, a typical value during the soft state of BHBs (McClintock & Remillard 2006), because the GSC energy band was dominated by the direct disk emission and hence Γ of the `simpl` model was poorly constrained. We confirm that adopting Γ values of from 2.2 to 2.7, instead of 2.50, does not affect our results. When the HR (8–20 keV vs 2–8 keV) is higher than 0.20, a single `powerlaw` model with free Γ was used instead of the `simpl*diskbb` model, because in their spectra the `diskbb` component cannot be constrained by the GSC data.

The inner disk radius $R_{\rm in}$ was estimated from the normalization of the `diskbb` component, by applying a correction factor of $\xi\kappa^2 = 1.18$, which is obtained by combining an adjustment to express stress-free boundary condition ($\xi = 0.41$: see, e.g., Kubota et al. 1998) with the color hardening factor ($\kappa = 1.7$; see, e.g., Shimura & Takahara 1995).

Figure 3 and table 1 present the spectra and the best-fitting models for representative spectra in the individual phases. Analyzing all the spectra in the same say, we have obtained successful fits from most of them. The long-term evolution of the derived best-fitting parameters is given in figure 4. For $T = 16$–25, 42–45, and 55–202, the $R_{\rm in}$ value, calculated assuming a distance $D = 10$ kpc, stayed fairly constant, in spite of significant variations of the flux, Comptonized fraction, and the inner disk temperature. In contrast, $R_{\rm in}$ increased and varied significantly for $T = 45$–53, where rapid spectral hardening occurred. The results generally confirm our state assignments employed so far; H1 and H2 as the hard state and S1 and S2 as the soft state.

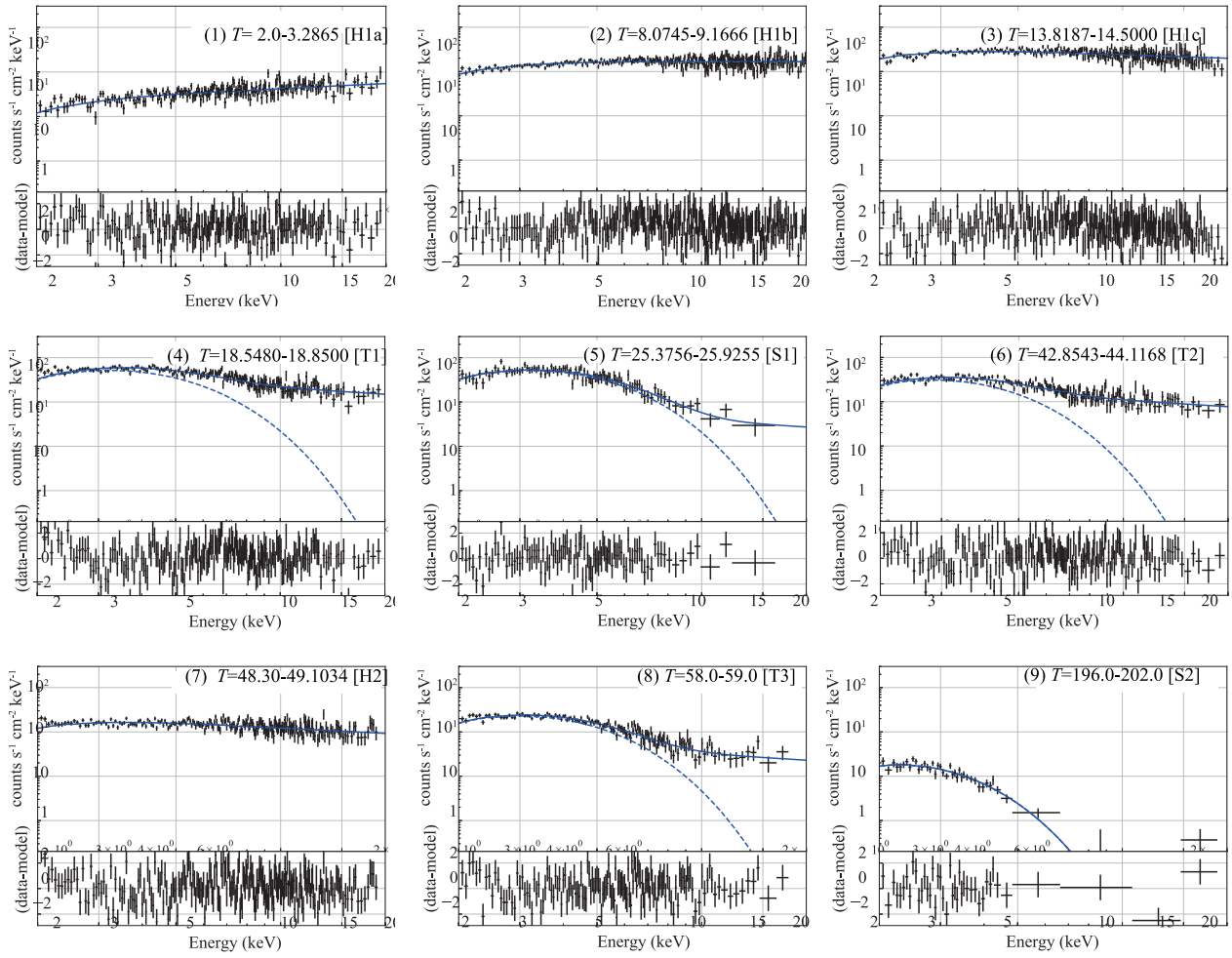

Fig. 3. Representative MAXI/GSC spectra in the individual phases (given in square brackets). The solid line shows the total model spectrum, and the dashed line indicates the intrinsic disk contribution. (Color online)

Table 1. Best-fitting model parameters obtained from the MAXI/GSC spectra.

Time [phase]	Flux*	Γ	$F_{\rm scat}{}^{\dagger}$	$T_{\rm in}$	$R_{\rm in}{}^{\ddagger}$	χ^2/d.o.f.
2.0000–3.2865[H1a]	1.33 ± 0.05	1.58 ± 0.06	—	—	—	1.00(182)
8.0745–9.1666[H1b]	6.08 ± 0.09	2.00 ± 0.03	—	—	—	1.02(284)
13.8187–14.5000[H1c]	10.14 ± 0.15	2.26 ± 0.03	—	—	—	1.12(256)
18.5480–18.8500[T1]	$15.62^{+0.31}_{-0.30}$	2.50 (fixed)	$0.21^{+0.03}_{-0.02}$	$1.00^{+0.04}_{-0.06}$	$99.15^{+13.49}_{-8.09}$	1.106(193)
25.3756–25.9255[S1]	$10.87^{+0.43}_{-0.50}$	2.50 (fixed)	0.02 ± 0.02	0.99 ± 0.06	$96.32^{+16.83}_{-13.59}$	0.790(96)
42.8543–44.1168[T2]	8.76 ± 0.20	2.50 (fixed)	0.18 ± 0.02	$0.83^{+0.04}_{-0.05}$	$116.97^{+18.99}_{-12.22}$	1.110(167)
48.30–49.1034[H2]	5.64 ± 0.10	2.38 ± 0.04	—	—	—	1.236(231)
58.0–59.0[T3]	$5.19^{+0.12}_{-0.11}$	2.50 (fixed)	0.07 ± 0.01	0.92 ± 0.03	$86.14^{+7.08}_{-7.07}$	1.05(144)
196.0–202.0 [S2]	$0.24^{+0.02}_{-0.01}$	$0.00^{+2.50}_{-2.50}$	$0.00^{+0.02}_{-0.00}$	$0.53^{+0.02}_{-0.06}$	$74.37^{+32.09}_{-7.92}$	1.115(39)

*2–20 keV X-ray flux in the units of $\times 10^{-8}$ erg cm^{-2} s^{-1}.
†Scattering fraction.
‡Inner radius estimated from the normalization of `diskbb` by assuming a distance and inclination of 10 kpc and 0°, respectively.

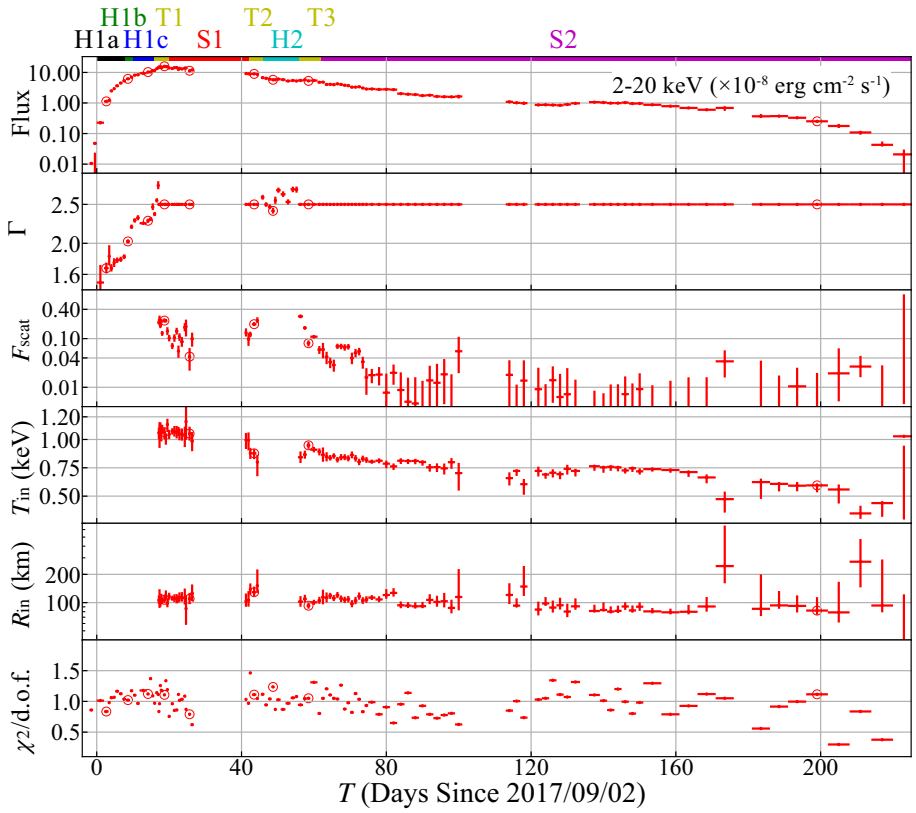

Fig. 4. Time evolution of the spectral parameters derived from the model fits to the 2–20 keV MAXI/GSC data. (Color online)

3 Discussion

3.1 Overall properties of the outburst

We have observed a dramatic outburst of MAXI J1535−571, with a peak X-ray intensity of ∼5 Crab, which is the seventh highest value among those of BH candidates observed so far. The source reached the outburst peak more than two weeks after the discovery, which is relatively long compared with the typical flux-rise time scales in BH candidates. Assuming a typical distance of $D = 10$ kpc and an isotropic emission, the 2–20 keV peak luminosity is obtained as $\sim 2.0 \times 10^{39}$ erg s^{-1}, which is comparable to the Eddington luminosity of a 10 $M_\odot$ BH where $M_\odot$ is the solar mass. Further discussion is provided later.

The evolution of the 2–20 keV flux is roughly characterized by a simple function of time, with a linear increase until $T = 18.5$ followed by an exponential decay and a re-flaring around $T = 130$. Meanwhile, its energy spectra exhibited sequential changes as shown in figure 3. In the following, we examine the spectral evolution.

At the beginning, MAXI J1535−571 brightened monotonically, accompanied by an increase of the photon index from $\Gamma \sim 1.5$ to ∼2.0 (H1a through H1c), and then rapidly softened through the transition T1, to reach the soft state S1. Subsequently, it gradually declined in ∼180 d with a decrease of $T_{\rm in}$ from ∼1 keV to 0.55 keV. However, during that course, it suddenly exhibited a spectral hardening (T2), stayed in a presumably hard state (H2) for about 10 days, and jumped back (T3) to the soft state (S2) to continue its decline. In H1c [$T = 10$–16; figure 3(3)] and H2 [$T = 46$–56; figure 3(7)], the source stayed in a state of flat spectrum for fairly long times, with $\Gamma \simeq 2.0$ (equivalent to HR of 0.2–0.4), even though the HR changed widely from ∼0.8 down to 0.01. The source declined rapidly after $T \sim 200$ (Negoro et al. 2018). After $T = 220$, the source became undetectable with the MAXI/GSC, with a typical detection limit of 3.0×10^{-10} erg cm^{-2} s^{-1} in 2–20 keV. Then, a spectral hardening was reported in the Swift/XRT observation at $T = 242$ (Russell et al. 2018). The overall behavior in the spectral evolution of MAXI J1535−571 supports the assumption that it is a BHB, although there are some characteristics unique to this source, including, as described below, the transition luminosity from the soft state back to the hard state.

In figure 4, the latest MAXI/GSC data point ($T = 214$–220) gives the lowest 2–20 keV X-ray flux during the decay phase, $\sim 0.04 \times 10^{-8}$ erg cm^{-2} s^{-1}, which corresponds to 0.25% of the peak flux (15.7×10^{-8} erg cm^{-2} s^{-1}). On that occasion, the source still remained in the soft state. At $T = 242$, however, the Swift spectrum was described with a

power-law model with $\Gamma \sim 1.6$, meaning that the source finally returned to the hard state. The 3–7 keV flux at that time, 2.2×10^{-12} erg cm^{-2} s^{-1}, is converted to the 2–20 keV flux of $\sim 6.4 \times 10^{-12}$ erg cm^{-2} s^{-1}, or 4×10^{-5} of the peak flux. This is unusually low compared with typical thresholds, $\sim$10% of the peak flux, observed in outburst of BHBs, such as XTE J1752–223 (Nakahira et al. 2012), MAXI J1659−152 (Yamaoka et al. 2012), and MAXI J1910−057 (Nakahira et al. 2014). This means that the transition in MAXI J1535−571 to the hard state occurred at much lower luminosity than in other BHBs, or that its peak luminosity was much higher than those of the others, both in terms of Eddington ratio.

3.2 Interpretation of the behavior on the HID

As in many black hole transients, we can clearly see hysteresis patterns in the HID (figure 2), on which the source roughly draws a counter-clockwise track. However, the track is split into two parts by an excursion to the hard state H2 as T2→H2→T3, which occurred when the luminosity decreased by a factor of $\sim$3, from the peak value in T1 (which is considered to be close to Eddington limit; subsection 3.3). Interestingly, the softest phase in the upper section (S1) has a spectrum similar to the softest spectrum in the lower section (S2), both dominated by the disk blackbody component, with similar $R_{\rm in}$ but different $T_{\rm in}$. However, as is clear by comparing spectra (5) and (9) in figure 3 and inspecting figure 4, the power-law contribution (represented by $F_{\rm scat}$) is considerably higher in S1 than in S2, where $F_{\rm scat}$ was a few percent like in typical BHBs in the soft state. In addition, the power-law component in S1 exhibited the noticeable variability (figure 1b, subsection 2.2). Therefore, S1 and S2 could be somewhat different.

A pattern on the HID, similar to that of MAXI J1535−571, is found in figure 4 of Belloni and Motta (2016) as "generic HID." According to these authors, our H1c and H2 could be classified as the hard–intermediate state, while S1 could be the soft–intermediate state. Clues to a more conclusive classification of the spectral states would be provided by spectral shapes above 10 keV, and the short-term flux variability; these are left as future studies using the present data.

In H1c and T1, the 2–8 keV and 15–50 keV fluxes showed small, repetitive fluctuations on a timescale of $\sim$ one day, with a sign of an anti-correlation (figure 1b; subsection 2.2). The time-averaged spectra in H1c have a fairly flat profile, characterized by a single power-law component. Thus, the anti-correlated flux variation would be produced by variations of the spectral index with a pivot energy at $\sim$10 keV. However, the low statistics of the MAXI data hampered us in detecting significant spectral differences at different phases of the fluctuation.

An intensity variation on a similar timescale was observed previously from MAXI J1659−152, but it has several different properties from that of MAXI J1535−571. The variation in MAXI J1535−571 was observed near the flux peak, whereas that of MAXI J1659−152 was observed in the decaying phase of an outburst. Moreover, the case of MAXI J1659−152 is characterized by positive correlations between the soft and hard signals, and hence it was suggested as being produced by precession of the accretion disk induced by a 3 : 1 resonance of its orbital period Kuulkers et al. (2013). The origin of the peculiar behavior in MAXI J1535−571 is hence still unclear, but could be associated with some changes in the structure of the Comptonized corona, in response to fluctuations of the mass accretion rate. A slight increase/decrease of the mass accretion rate would cause an increase/decrease of the number of seed photons for Comptonization in the corona, and thereby the corona could be cooled/heated, leading to a change in the Comptonized continuum (e.g., Shidatsu et al. 2014).

3.3 Constraint on the black hole mass

For $T = 16$–25 (T1 to S1) and $T = 55$–202 (T3 to S2) in figure 4, $R_{\rm in}$ remained relatively constant at an average of 101 $(D/10\,{\rm kpc})$ $(\cos i/\cos 0)^{-1/2}$ km, despite the large flux change over nearly two orders of magnitude. Therefore, in these periods, the inner edge of the standard disk is likely to have reached the innermost stable circular orbit (ISCO). Now that the ISCO information has been obtained as above, let us constrain the black hole mass $M_{\rm BH}$ of MAXI J1535−571, utilizing a D versus $M_{\rm BH}$ diagram in figure 5. There, a pair of solid black lines were obtained by identifying the observed disk radius, $R_{\rm in} = 101\ (D/10\,{\rm kpc})\ (\cos i/\cos 0)^{-1/2}$ km, with the ISCO of a Schwarzschild BH, namely, three times the Schwarzschild radius. Here, i is the disk inclination, which is assumed to be $i = 0^\circ$ and 60°. The red dashed lines represent the condition that the outburst peak luminosity $L_{\rm peak}$ corresponds to 10%, 20%, 50%, and 100% of $L_{\rm edd}$. In order for $M_{\rm BH}$ to fall in a typical mass range of 5–15 $M_\odot$ (McClintock & Remillard 2006), the ratio $L_{\rm peak}/L_{\rm edd}$ should be higher than, say, several tens of percent.

In the above estimates, we assumed a Schwarzschild black hole, which may not be realistic. If the BH is spinning considerably, as suggested by Xu et al. (2018) by modeling the reflection feature in the NuSTAR spectrum of this object, the ISCO radius should decrease, down to $\sim$0.5 Schwarzschild radii at the extreme. Furthermore, the disk spectrum would be more strongly affected by relativistic

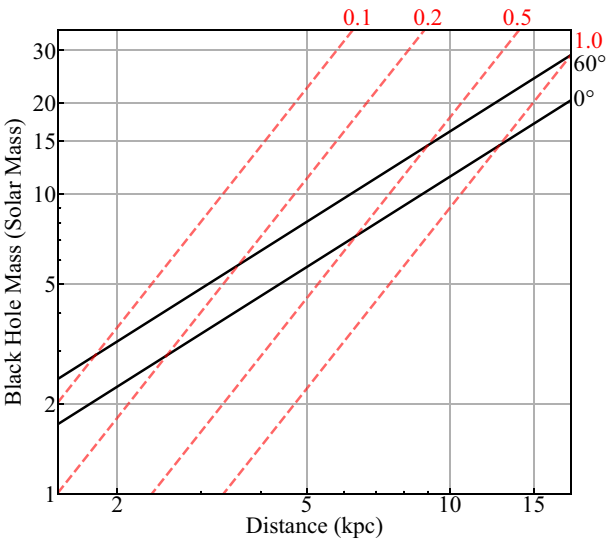

Fig. 5. Distance–mass diagram of MAXI J1535−571, with two sets of observational constraints. Black lines show those obtained by identifying the observed values of $R_{\rm in}$ with ISCO of Schwarzschild BHs, whereas red dashed lines give constraints by estimating the Eddington limits from the observation. The associated numbers in red indicate the assumed $L_{\rm peak}/L_{\rm edd}$ ratio. (Color online)

effects. However, the NuSTAR data were acquired at $T = 5.78$, or at a phase H1a in our data, when the object was clearly in the hard state. It is not clear to us whether the disk in the hard state can really get so close (<2.1 times the ISCO radius; Xu et al. 2018) to the central BH, considering that the disk in the hard state is usually observed to truncate at radii considerably larger than ISCO (Shidatsu et al. 2011). Since the the MAXI/GSC data are limited in statistics, applying a relativistic disk emission model may not give meaningful constraints on the BH spin. This is also left for our future studies.

4 Summary and conclusions

Using the MAXI/GSC, we monitored the X-ray spectral evolution of the particularly bright black hole binary MAXI J1535−571, from the onset of its outburst until the source faded below the detection limit at $T > 220$.

(1) On the hardness vs. 2–20 keV intensity diagram, the source showed a hysteresis behavior, by exhibiting a few transitions between the hard state and the soft state. During the decline phase in the soft state at the 30%–40% of the peak luminosity it made an excursion to the relatively hard state for ∼10 d.

(2) When the source was in the hard state, prior to the excursion, it exhibited quasi-periodic fluctuations on a time scale of ∼1 d, with an amplitude of 10%–20% and a clean anti-correlation between 2–8 keV and 15–50 keV. This is likely to be caused by slope changes in the power-law component, which dominated the spectrum at that epoch.

(3) The MAXI/GSC energy spectrum can be fitted by a single power-law, or a Comptomized disk blackbody model. From the peak to almost the end, the innermost disk temperature and the 2–20 keV X-ray flux was observed to decrease from 1.2 to 0.5 keV, and from 15.7×10^{-8} erg cm^{-2} s^{-1} to 0.04×10^{-8} erg cm^{-2} s^{-1}, respectively. Meanwhile, the innermost disk radius stayed relatively constant at $101\,(D/10\,{\rm kpc})(\cos i/\cos 0^\circ)^{-1/2}$ km.

Acknowledgments

This research has made use of MAXI data provided by RIKEN, JAXA and the MAXI team. Part of this work was financially supported by Grants-in-Aid for Scientific Research 16K17672 (MS), 16K05301 (HN) and 17H06362 (YU, TM, HN, and NK) from the Ministry of Education, Culture, Sports, Science and Technology (MEXT) of Japan. MS acknowledges support by the Special Postdoctoral Researchers Program at RIKEN.

References

Belloni, T. M., & Motta, S. E. 2016, in Astrophysics of Black Holes: From Fundamental Aspects to Latest Developments, ed. C. Bambi (Berlin: Springer-Verlag), 61
Britt, C. T., Bahramian, A., & Strader, J. 2017, Astronomer's Telegram, 10816
Dincer, T. 2017, Astronomer's Telegram, 10716
Done, C., Gierliński, M., & Kubota, A. 2007, A&AR, 15, 1
Gendreau, K., Arzoumanian, Z., Markwardt, C., Okajima, T., & Strohmayer, T. 2017, Astronomer's Telegram, 10768
Hiroi, K., et al. 2013, ApJS, 207, 36
Homan, J., & Belloni, T. 2005, Ap&SS, 300, 107
Kennea, J. A. 2017, Astronomer's Telegram, 10731
Kennea, J. A., Evans, P. A., Beardmore, A. P., Krimm, H. A., Romano, P., Yamaoka, K., Serino, M., & Negoro, H. 2017, Astronomer's Telegram, 10700
Krimm, H. A., et al. 2013, ApJS, 209, 14
Kubota, A., Tanaka, Y., Makishima, K., Ueda, Y., Dotani, T., Inoue, H., & Yamaoka, K. 1998, PASJ, 50, 667
Kuulkers, E., et al. 2013, A&A, 552, A32
McClintock, J. E., & Remillard, R. A. 2006, in Compact Stellar X-ray Sources, ed. W. H. G. Lewin & M. van der Klis (New York: Cambridge University Press), 157
Markwardt, C. B., Burrows, D. N., Cummings, J. R., Kennea, J. A., Marshall, F. E., Page, K. L., Palmer, D. M., & Siegel, M. H. 2017, GCN Circ., 21788
Matsuoka, M., et al. 2009, PASJ, 61, 999
Mereminskiy, I. A., & Grebenev, S. A. 2017, Astronomer's Telegram, 10734
Mitsuda, K., et al. 1984, PASJ, 36, 741
Nakahira, S., et al. 2012, PASJ, 64, 13
Nakahira, S., et al. 2017, Astronomer's Telegram, 10729
Nakahira, S., Ebisawa, K., Negoro, H., Mihara, T., Sugizaki, M., Serino, M., Suwa, F., Asada, M., & Tomida, H. 2013, J. Space Sci. Informatics, 2, 29

Nakahira, S., Negoro, H., Shidatsu, M., Ueda, Y., Mihara, T., Sugizaki, M., Matsuoka, M., & Onodera, T. 2014, PASJ, 66, 84
Negoro, H., et al. 2016, PASJ, 68, S1
Negoro, H., et al. 2017a, Astronomer's Telegram, 10699
Negoro, H., et al. 2017b, Astronomer's Telegram, 10708
Negoro, H., et al. 2018, Astronomer's Telegram, 11568, 1
Palmer, D. M., Krimm, H. A., & Swift/BAT Team 2017, Astronomer's Telegram, 10733
Russell, T. D., Altamirano, D., Tetarenko, A. J., Sivakoff, G. R., Neilsen, J., Miller-Jones, J. C. A., van den Eijnden, J., & Jacpot Xrb Collaboration 2017a, Astronomer's Telegram, 10899
Russell, T. D., Miller-Jones, J. C. A., Sivakoff, G. R., Tetarenko, A. J., & Jacpot Xrb Collaboration 2017b, Astronomer's Telegram, 10711
Russell, T. D., Rapisarda, S., Altamirano, S. R. D., Miller-Jones, J. C. A., Plotkin, R., Tetarenko, A. J., Sivakoff, G. R., & JACPOT XRB Collaboration 2018, Astronomer's Telegram, 11611
Scaringi, S., & ASTR211 Students 2017, Astronomer's Telegram, 10702
Shidatsu, M., et al. 2011, PASJ, 63, S785
Shidatsu, M., et al. 2017, Astronomer's Telegram, 10761
Shidatsu, M., Ueda, Y., Yamada, S., Done, C., Hori, T., Yamaoka, K., Kubota, A., Nagayama, T., & Moritani, Y. 2014, ApJ, 789, 100
Shimura, T., & Takahara, F. 1995, ApJ, 445, 780
Steiner, J. F., Narayan, R., McClintock, J. E., & Ebisawa, K. 2009, PASP, 121, 1279
Tetarenko, A. J., Russell, T. D., Miller-Jones, J. C. A., Sivakoff, G. R. & Jacpot Xrb Collaboration 2017, Astronomer's Telegram, 10745
Wilms, J., Allen, A., & McCray, R. 2000, ApJ, 542, 914
Xu, Y., et al. 2018, ApJ, 852, L34
Yamaoka, K., et al. 2012, PASJ, 64, 32